Journal of Chromatography A, 1218 (2011) 5504–5511

Contents lists available at ScienceDirect

Journal of Chromatography A

journal homepage: www.elsevier.com/locate/chroma

High-resolution separations of protein isoforms with liquid chromatography time-of-flight mass spectrometry using polymer monolithic capillary columns

Sebastiaan Eeltink[a,*], Bert Wouters[a], Gert Desmet[a], Mario Ursem[b], David Blinco[c], Glenwyn D. Kemp[c], Achim Treumann[c]

[a] Vrije Universiteit Brussel, Department of Chemical Engineering, Pleinlaan 2, B-1050 Brussels, Belgium
[b] Dionex Corporation, Abberdaan 114, 1046 AA Amsterdam, The Netherlands
[c] NEPAF, North East Proteome Analysis Facility, Devonshire Building, Newcastle upon Tyne, United Kingdom

ARTICLE INFO

Article history:
Received 21 March 2011
Received in revised form 16 May 2011
Accepted 10 June 2011
Available online 21 June 2011

Keywords:
Top-down proteomics
Protein isoforms
Monolithic columns
ABRF proteomics standard

ABSTRACT

The separation of intact proteins, including protein isoforms arising from various amino-acid modifications, employing a poly(styrene-*co*-divinylbenzene) monolithic capillary column in high-performance liquid chromatography coupled on-line to a time-of-flight mass spectrometer (MS) is described. Using a 250 mm × 0.2 mm monolithic capillary column high-sensitivity separations yielding peak capacities of >600 were achieved with a 2 h linear gradient and formic acid added in the mobile phase as ion-pairing agent. The combination of high-resolution chromatography with high-accuracy MS allowed to distinguish protein isoforms that differ only in their oxidation and biotinylation state allowing the separation between structural isoforms. Finally, the potential to separate proteins isoforms due to glycosylation is discussed.

1. Introduction

The mainstay of the successful mass-spectrometry (MS) based proteomics in the past 15 years is the so-called bottom-up approach to proteomics. It is based on the proteolytic digest of proteins in gel or in solution, followed by chromatographic separation and mass-spectrometric identification of the peptide ions by matrix-assisted laser desorption/ionization-time of flight (MALDI-TOF) or electrospray ionization (ESI) MS [1,2]. The introduction of high-resolution mass spectrometers and of new fragmentation techniques has resulted in the increased interest in top-down approaches to proteomics [3,4]. MS-based top-down proteomics is based on the chromatographic separation of intact proteins followed by their fragmentation in the gas phase using collision-induced dissociation (CID) [5,6], electron-capture dissociation (ECD) [7,8] or electron-transfer dissociation (ETD) [9,10].

Top-down approaches are attractive, because they have the potential to supply information about the modifications of the analyzed proteins, resolving isoforms that are frequently unresolved in bottom-up proteomics experiments, including isoforms resulting from proteolytic processing, oxidative damage, glycosylation, or other forms of post-translational processing. The two main prerequisites for successful top-down proteomics are high-resolution chromatography and high sensitivity and high-resolution mass spectrometry with fragmentation possibilities. To achieve their full potential, top-down workflows have to overcome several challenges: (1) chromatographic separation of complex mixtures of the intact proteins, (2) fragmentation of the proteins in the gas-phase, (3) sensitivity of detection for the intact proteins, and (4) data analysis of the complex MS/MS spectra.

For the separation of intact proteins, reversed-phase liquid chromatography (RPLC) has often been employed, due to excellent solvent compatibility with electrospray interfacing prior to MS detection. However, low protein recovery has frequently been a problem associated with this approach [11]. Polymer monolithic stationary phases have shown great potential for RPLC separations of large biomolecules, including intact proteins [12–15], oligonucleotides [16,17], and peptides [18–20]. Conceptually, this material is very well suited to perform large-molecule gradient-separations since mass transfer is mainly driven by convection, rather than by diffusion due to the absence of mesopores (stagnant zones in microglobules) [21]. In addition, Kelleher et al. demonstrated that polymeric stationary phases led to superior sensitivity over silica-based media in reversed-phase nanocapillary LC, with detection of proteins >50 kDa [22].

Polymer monoliths from styrene and divinylbenzene were initially developed by Svec and coworkers in large I.D. column formats for the separation of styrene oligomers and polymers based on precipitation–redissolution chromatography [23]. Similar materials have more recently been used for the extracts of intact

* Corresponding author. Tel.: +32 02 629 3324, fax: +32 02 629 3248.
E-mail address: seeltink@vub.ac.be (S. Eeltink).

0021-9673/$ – see front matter © 2011 Elsevier B.V. All rights reserved.
doi:10.1016/j.chroma.2011.06.049

membrane proteins containing antenna or/and core proteins [24]. RPLC–MS was performed by applying linear 20–40 min acetonitrile gradients containing 0.05% trifluoroacetic acid and identification was based on comparison of the measured intact mass of the protein and the theoretical relative molecular weight (M_r) values. To achieve full baseline separation between 12 core proteins present in spinach, column temperatures up to 78 °C were applied. A disadvantage of applying higher temperatures is that proteins may be prone to degradation, *i.e.* intra-molecular disulfide bonds may be broken and the amide backbone of the proteins may be hydrolyzed, making protein identification based on the comparison of the experimentally determined and theoretical molecular weight difficult [25]. This separation example shows the need for monolithic columns with improved morphology and the development of longer monolithic columns providing better separation performance at mild LC conditions. Recently, we demonstrated the use of a 50 mm long poly(styrene-*co*-divinylbenzene) monolithic 1 mm I.D. column for the separation of intact proteins [26]. When applying a 1 min gradient peak widths at half height of only 1 s were achieved. At longer gradient duration (120 min) a maximum peak capacity of 475 was observed [26]. Using a 50 mm long capillary poly(styrene-*co*-divinylbenzene) monolith coupled to a LTQ Orbitrap XL mass spectrometer a limit of detection in the low femtomol range was achieved using a standard mixture of nine proteins with a molecular weight ranging between 5.7 and 150 kDa [27]. Using the developed LC–MS method, the 70% ethanol-soluble subproteome of wheat grains was analyzed and 53 different protein masses were obtained from 26 extracted mass spectra. However, it was concluded that identification by comparison of measured molecular masses with masses derived from the published sequences was not possible due to the high sequence homology of gliadins and high number of protein and gene sequences available in the databases. In an experimental study to investigate the effect of column parameters (morphology and length) and gradient time on the performance of capillary poly(styrene-*co*-divinylbenzene) monoliths, it was shown that when using long (250 mm) monolithic columns with optimized morphology a peak capacity of 620 could be achieved for the separation of intact proteins applying a 120 min gradient and UV detection [28].

The present paper discusses the potential of long poly(styrene-*co*-divinylbenzene) monolithic capillary columns for the gradient-elution LC–TOF-MS analysis of intact proteins, including protein isoforms. We address two aspects relevant to the top-down proteomics workflow, namely chromatographic separation at high resolution and MS sensitivity in the detection of the separated proteins. Experimental conditions, including ion-pairing agent (TFA *versus* FA) and gradient time, were adjusted and their effects on retention, peak widths, and signal-to-noise ratios are discussed. We demonstrate the high-resolution separation of a standard 48 protein mixture with low (sub-pmol) protein amounts. In addition, the potential of this set-up for the separation of protein isoforms arising from amino acid modifications is investigated, including oxidation and glycosylation.

2. Experimental

2.1. Chemicals and materials

Acetonitrile (ACN, HPLC supra-gradient quality), formic acid (FA, LC–MS quality), and trifluoroacetic acid (TFA, ReagentPlus quality) were purchased from Sigma–Aldrich (Dorset, United Kingdom). A "Universal Proteomics Standard 1" set was purchased from Sigma–Aldrich (Bornem, Belgium). This set was developed in collaboration with the Association of Biomolecular Resource Facilities (ABRF) Proteomics Standards Research Group (sPRG) (Maryland, USA) and is comprised of one vial containing 48 human source or human sequence recombinant proteins. The total protein content in the vial is 6 mg, which constitutes 5 pmol of each HPLC purified protein. Water was purified in-house using a Millipore Simplicity System (Millipore, Bedford, MA, USA).

A 5 mm × 0.2 mm PepSwift trap column and a 250 mm × 0.2 mm PepSwift RP monolithic columns were provided by Dionex Benelux (Amsterdam, The Netherlands).

2.2. Instrumentation and LC–MS conditions

LC–MS experiments were conducted using an UltiMate 3000 Proteomics MDLC system (Dionex Corporation, Germering, Germany) consisting of a dual-ternary gradient pump with membrane degasser, a thermostatted flow-manager module, and a well-plate autosampler, which was coupled on-line with a maXis ultra-high-resolution qTOF mass spectrometer with a nano-electrospray interface (Bruker Daltonics, Bremen, Germany) equipped with a Proxeon steel emitter.

The separations were performed using the "pre-concentration injection" set-up, with the trap column maintained outside the column oven and the monolithic separation column thermostatted in the oven at 60 °C. After partial-loop injection of 750 or 200 fmol/protein of the ABRF protein mixture, dissolved in water containing 0.02% FA, the sample was desalted on the trap column for 2 min at a flow rate of 20 μL/min and thereafter separated on the 250 mm long monolithic column applying an aqueous acetonitrile gradient from 8% B to 55% B (80% ACN) containing 0.02% FA or TFA at a flow rate of 1.5 μL/min. The chromatographic peak capacity (n_c) was determined applying Eq. (1), where t_G is the gradient time, and W the average 4 sigma peak width:

$$n_c = \frac{t_G}{W} + 1 \quad (1)$$

The data acquisition software was DataAnalysis software 4.0, SP1 (Bruker Daltonics). Spectra were obtained in positive ion mode using the following instrumental parameters: capillary voltage, 4.50 kV; nebulizer, 0.6 bar; dry gas rate, 4.0 L/min; dry gas temperature, 180 °C; funnel RF, 400 Vpp; multipole RF, 400 Vpp; ion energy, 5.0 eV; collision energy, 10.0 eV; collision RF, 1400 Vpp; ion cooler RF, 400 Vpp.

Extracted ion chromatograms (EICs) refer to chromatograms showing the trace of a specific mass (±0.5 Da), *e.g.* 1067.94 ± 0.5. EICs are calculated by summing up the intensities of all specified masses in the mass spectra. Spectra of multiply charged ions were interpreted using the deconvolution algorithms implemented in the instrument software package (DataAnalysis software Version 4, SP2, Bruker).

3. Results and discussion

3.1. Optimization of LC–MS conditions

The effect of ion-pairing agent on the chromatographic performance (retention time, peak width) and mass-spectrometric sensitivity of the gradient-elution LC–TOF-MS separation of intact proteins on the 0.2 mm × 250 mm monolithic capillary column is shown in Fig. 1. To compare the retention properties, both the gradient duration and gradient slope were kept constant throughout the experiments. Retention time, peak width at half height ($w_{1/2}$), and signal-to-noise (S/N) ratios were determined from extracted-ion chromatograms of proteins that elute evenly distributed over the 60 min gradient, see Table 1. No difference in selectivity was observed for the selected proteins. An increase in retention was observed when using 0.02% formic acid FA as ion-pairing agent in the mobile phase, as opposed to 0.02% trifluoroacetic acid (TFA).

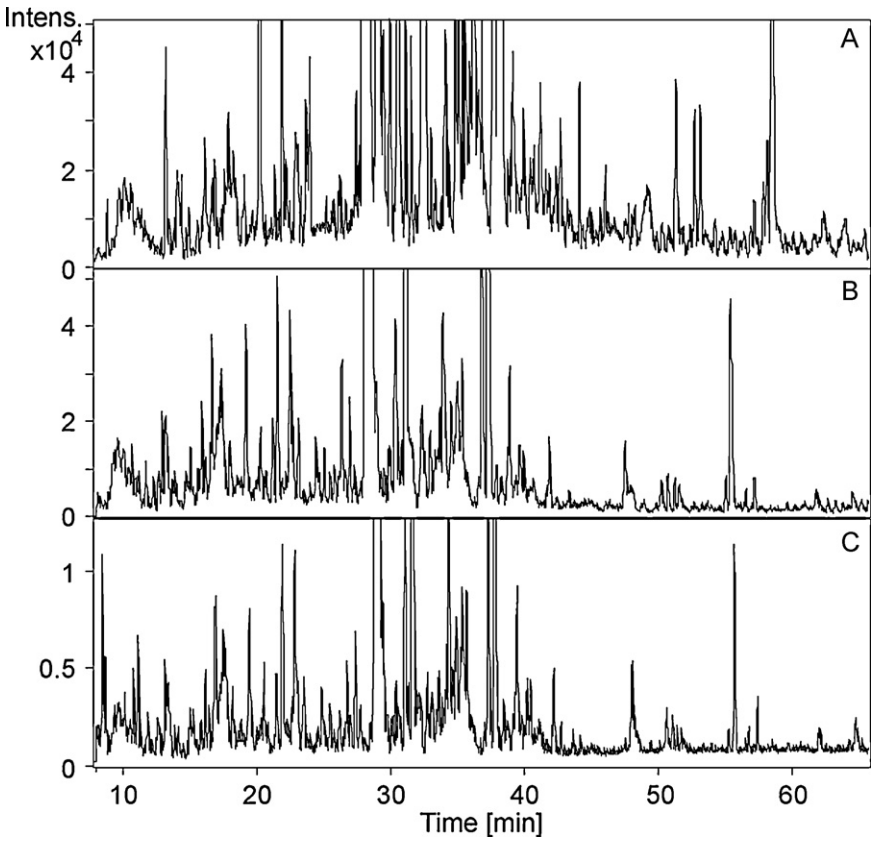

Fig. 1. Effect of ion-pairing agent on retention time, peak width, and MS sensitivity. Base-peak chromatograms applying a 60 min gradient with FA as ion-pairing agent, 750 fmol/protein injected (A), TFA as ion-pairing agent, 750 fmol/protein injected (B), and TFA as ion-pairing agent, 150 fmol/protein injected (C).

This effect was more pronounced for proteins eluting later during the gradient, resulting in a maximum shift in retention time of 5.5%.

When comparing the signal intensities of the base-peak chromatograms in Fig. 1A and B that have the same amount injected (750 fmol/protein) and visualized with a similar scale, it can be observed that the signal with FA as ion-pairing agent (Fig. 2A) is approximately 2.5–3 fold higher than when using TFA (Fig. 2B). This is mainly due to ion suppression by TFA. Still, when injecting only 200 fmol/protein and using TFA as ion-pairing agent (Fig. 1C) signal-to-noise ratio's determined from extracted ion chromatograms ranged between 322 (EIC = 1187.0 ± 0.5 m/z) and 11 (EIC = 1490.5 ± 0.5 m/z). Table 1 also shows the effect of ion-pairing agent on $w_{1/2}$ and the corresponding peak capacity (n_c), see Eq. (1) in Section 2. At a gradient time of 60 min, the average peak width with FA as ion-pairing agent was 12.9 s, whereas the peak width at half height with TFA was only 10.8 s. As a result, the average peak capacity is slightly higher when using TFA (211 *versus* 233 for FA and TFA, respectively).

For the characterization of the 48 protein mixture the LC–TOF-MS analysis was performed using FA as ion-pairing agent and applying a gradient time of 120 min, thereby increasing the resolution between the proteins [28]. At these conditions, the mass-spectrometric resolution (R_s) of the TOF mass spectrometer was determined at 29,452 for a low molecular-weight protein (IGF-II; relative molecular weight, M_r = 7468 Da), 29,655 for alpha-lactalbumin with M_r = 14,070 Da, and 26,854 for a peroxiredoxin 1 (M_r = 21,974 Da). Peak capacities of intact proteins were determined to be between 103 and 679 based on extracted ion chromatograms. Interesting to note is the variation in peak width, as illustrated in the extracted ion chromatograms in Fig. 2. The peak width determined at half height varied between 6 and 41 s. The presence of broad peaks can partly be explained by protein heterogeneity, such as glycosylated isoforms of serotransferrin (M_r = 79,554 Da) eluting between 90 and 94 min (Fig. 2B). In other cases heterogeneity in peak width is indicative of imperfect chromatographic behavior, *e.g.* interleukin-8 (M_r = 8381 Da) elutes as a broad peak (Fig. 2C).

Table 1
Retention times, peak widths, and signal-to-noise ratios estimated from extracted ion chromatograms of selected proteins separated on a 250 mm × 0.2 mm monolithic column applying a 60 min gradient with 0.02% FA or TFA added in the mobile phase, respectively.

M_r (Da)	FA					TFA				
	t_R (min)	EIC	$w_{1/2}$ (s)	n_c	S/N	t_R (min)	EIC	$w_{1/2}$ (s)	n_c	S/N
6251	13.169	894.05 (7+)	7.4	287	127	12.883	1042.89 (6+)	7.6	280	96
9488	21.543	1186.99 (8+)	5.5	384	43	21.128	1186.99 (6+)	5.9	357	20
8381	27.848	1048.68 (8+)	25.8	82	993	28.036	1397.83 (6)	20.3	104	714
7468	32.310	1067.93 (7+)	16.3	130	1141	31.008	1245.76 (6+)	13.7	155	684
11,729	37.981	1067.25 (11+)	17.1	124	1373	37.166	1067.25 (11+)	13.6	156	615
6641	44.006	949.79 (7+)	6.4	330	104	42.402	949.64 (7+)	5.8	368	12.6
17,871	51.195	1052.24 (17+)	10.9	194	218	50.611	1117.95 (16+)	8.6	247	96.8
1564	58.316	1564.30 (9+)	13.4	158	1592	55.276	2010.89 (7+)	10.9	195	186

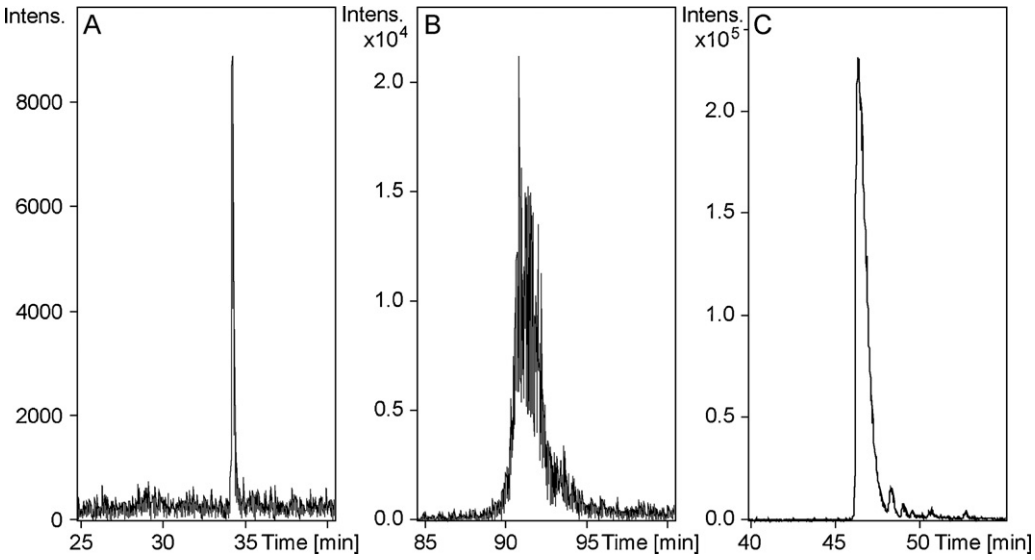

Fig. 2. Extracted-ion chromatograms demonstrating the difference in peak widths observed for three different proteins. (A) A homogeneous protein (M_r 9487 Da, EIC = 1186.99 ± 0.1 m/z), (B) a glycosylated heterogeneous protein (M_r 79,554 Da, EIC = 2040.90 ± 0.1 m/z) and (C) a homogeneous protein displaying an increased peak width (M_r 8381 Da, EIC = 1048.68 ± 0.1 m/z).

Fig. 3 shows the separation of the 48 protein mixture applying a gradient time of 120 min. A density-view plot (three-dimensional representation of the LC–TOF-MS analysis depicted in Fig. 3B) illustrates the chromatographic resolution (*abscissa*) and visualizes the different charge states of the proteins (*ordinate*). The color intensity (*z*-axis) represents the ion intensity. The advantage of this representation of the LC–TOF-MS is that co-eluting proteins can be distinguished, which is in clear contrast with a total ion chromatogram (TIC). This is for example the case for the proteins eluting between 90 and 94.5 min that co-elute in the TIC representation, but in the 3D plot five proteins can be distinguished.

Protein identification was based on deconvolution of charge envelopes in mass spectra followed by matching of experimentally determined M_r values with theoretical values. Fig. 4A shows the charge envelope of a protein eluting at 67.3 min with a S/N ratio determined from its EIC of 1263 m/z. The most abundant charge state was determined at 11+, and the average molecule weight (M_r) after deconvolution was determined at 11,729 Da. This mass corresponds to the molecular weight of beta-2-microglobulin with a theoretical M_r of 11,731 Da. The mass difference of 2 Da can be explained by the formation of a disulfide bridge, which is a documented post-translational modification for this particular protein. Fig. 4B shows the zoom-in of the most abundant charge state (11+) of beta-2-microglobulin demonstrating isotopic resolution. Fig. 4C shows the mass spectrum of two co-eluting proteins at t_R = 89.4 min with a signal-to-noise ratio of 20–40. The charge envelope at high m/z (marked with asterisks) depicts a protein with the most abundant charge state of 11+, with a M_r of 20,568 Da. The protein marked with black crosses depicts a protein with M_r = 34,102 (most abundant charge state is 34+). These proteins most likely correspond to ubiquitin-conjugating enzyme E2 C and annexin A5, respectively. Fig. 4C clearly shows the need for high-resolution columns in order to distinguish different protein charge envelopes, particularly for the prevention of ion-suppression effects that are expected for co-eluting proteins.

Despite of the use of a high-resolution TOF mass-spectrometer it should be emphasized that protein identifications can only be tentative. Experimental molecular weight values may differ from the theoretical values, for example, due to alternative splicing and the presence of co- and post-translational modifications (PTMs). In addition, although the ABRF protein mixture was intended to contain 48 proteins, the ABRF Proteomics Standards Research Group Bioinformatics Committee has confirmed the presence of 'bonus' proteins [29]. A table listing all the experimentally determined M_r values and corresponding retention times, and tentative identification (protein name, protein tag, potential PTMs, and UniProt accession number) and the mass spectra depicting the charge envelopes of the different proteins is supplied as Supporting Information. In total, 30 different protein masses (57 charge envelopes including protein isoforms) were obtained from the 120 min gradient run depicted in Fig. 3. Based on mass alone, 24 charge envelopes could be tentatively assigned to proteins that are known to be in the 48 protein mixture.

3.2. Separation and characterization of protein isoforms

Fig. 5A shows a zoom-in of the three-dimensional representation of proteins eluting between 96 and 99 min. The similarity between the charge envelopes is indicative of the elution of protein isoforms that are baseline separated. The experimentally determined M_r values coincide well with the mass of peroxiredoxin 1 (MW = 21,979). Peroxiredoxin I belongs to a family of anti-oxidant enzymes that control cytokine-induced hydrogen peroxide levels in cells [30]. When exposed to peroxide, the redox-active Cys-52 is oxidized to Cys-OH, which rapidly reacts with Cys-173-SH to form an intermolecular disulfide bridge. Overoxidation of peroxidatic cysteine may occur in the presence of thioredoxin yielding sulfinic (Cys-SO_2H) or sulfonic (Cys-SO_3H) acid forms [30]. In addition, peroxiredoxin 1 contains three methionine molecules that are prone to oxidation.

In the zoom-in with m/z ranging between 1156 and 1160 depicted in Fig. 5B different protein isoforms can be distinguished. After mass deconvolution of the charge envelopes of peaks 6–10, a M_r value of 21,990 Da was obtained. The M_r value of peaks 3–5 was determined at 21,974 Da. The mass difference of 16 Da between the two M_r values experimentally found is indicative for protein oxidation. The distance in the *y*-direction between peaks 6–10 and peaks 3–5 that differ in oxidation state (ΔM = 16 Da) is approximately similar as the distance between peaks 3–5 and peaks 1–2 (Fig. 5B). Therefore, it is likely that this difference in charge state is also induced by oxidation. We speculate that the native peroxiredoxin I is represented by the cluster of peaks 1–2. Peaks 3–5 may represent

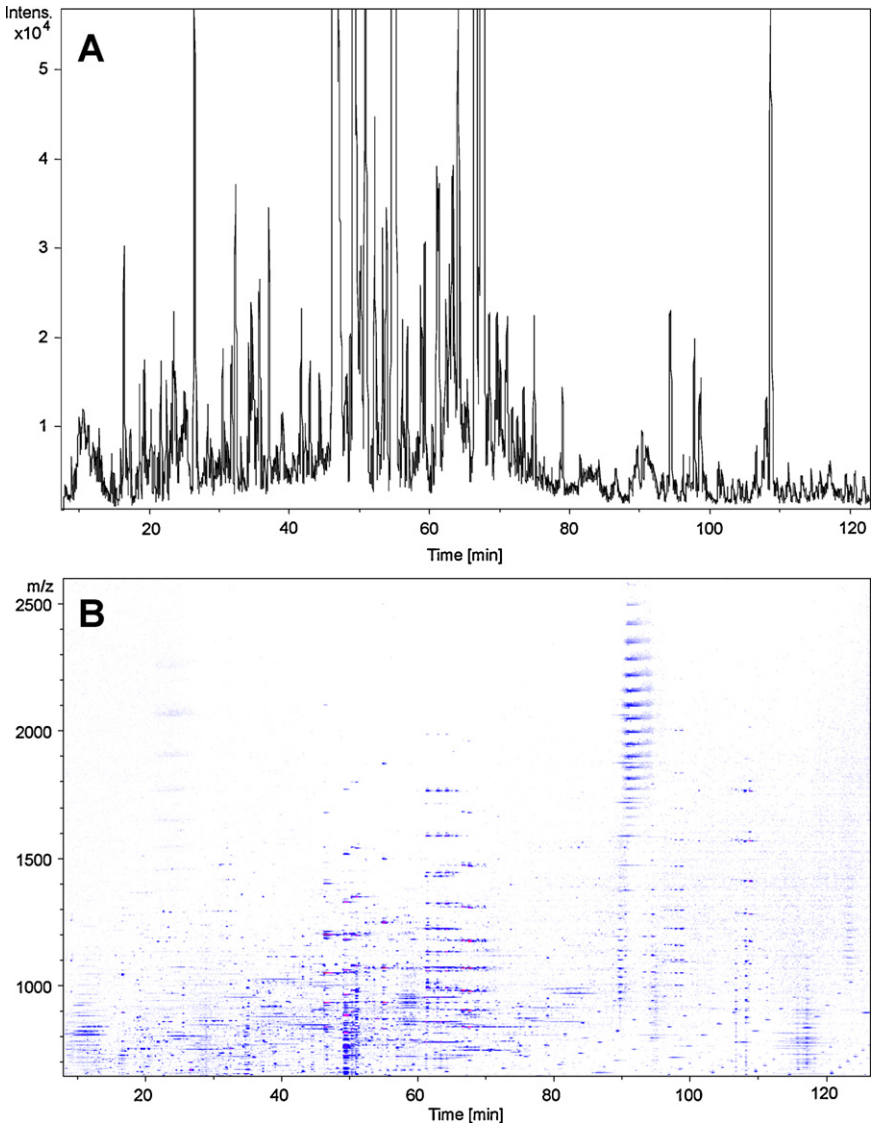

Fig. 3. LC–TOF-MS analysis of a 48 intact protein mixture on a 250 mm × 0.2 mm monolithic column applying a 120 min gradient. (A) The total ion chromatogram and (B) the density-view representation. 1 μL injection, 750 fmol/protein, 0.02% FA added in mobile-phase as ion pairing agent, flow rate 1.5 μL/min.

singly oxidized peroxiredoxin I protein isoforms. It is likely proteins that are oxidized at different sites, *i.e.* cysteine and methionine oxidation may results in a different tertiary structure of the proteins. Hence retention factors between singly oxidized species may differ and a separation between singly oxidized isoforms is obtained. The five protein isoforms (peaks 6–10) may contain two oxidations. The extracted ion chromatograms of singly (EIC $1157.5 \pm 0.5\ m/z$) and doubly oxidized isoforms (EIC $1158.3 \pm 0.5\ m/z$) are shown in Fig. 5C and D, respectively. The $w_{1/2}$ ranged between 7.8 and 12.3 s. With increasing oxidation state a shift to lower retention times is observed, which is in agreement with the fact that the protein becomes more polar. It is interesting to observe that single and double oxidations occurring in different places in the peroxidase appear to cause differences in retention time. This could be explained either by effects of direct interactions of the oxidized sequence with the stationary phase or by changes of the tertiary structure of the protein.

Fig. 6A shows the density view plot of protein isoforms eluting between 107 and 110 min. The experimentally determined M_r value of 14,069.7 Da with a charge state of 9+ eluting at 108.5 min corresponds with the molecular weight of alpha-lactalbumin (14,070 Da). Alpha-lactalbumin is a known glycoprotein that acts as a regulatory subunit of lactose synthase. The mass difference of 326 Da between peaks 1–2 and 2–3 in Fig. 6B corresponds to the addition of one and two N-(biotinoyl)-N″-(iodoacetyl)ethylenediamine residues (326.1 Da), respectively. Biotin tags are widely used enabling the isolation of target proteins via affinity chromatography [31]. The mass difference of 16 Da observed between peaks 1–4, 4–6, and 2–5 indicates protein oxidation of a methionine or cysteine residue. Also, a shift to lower retention time is observed, further confirming the addition of a polar group. The mass difference between peaks 1–7 of 162.5 Da may be explained by the addition of a hexose monosaccharide residue, as a result of a Maillard reaction. The cluster of peaks eluting at 108.5 min with a m/z ranging from 1565 to 1575 could represent the exchange of amino acids.

Fig. 3 shows a broad peak at high mass-to-charge ratio eluting between 89 and 95 min. In contrast to peroxiredoxin I, where different protein isoforms elute as narrow bands, the magnification in Fig. 7A shows highly scattered data in both x and y-directions. This indicates the elution of a very heterogeneous protein(s). In the zoom-in mass spectrum different isoforms become apparent, with M_r values ranging between 79,265 and 79,864 Da. The strongest signal in the mass spectrum (peak 2) has a M_r value of 79,555 Da with

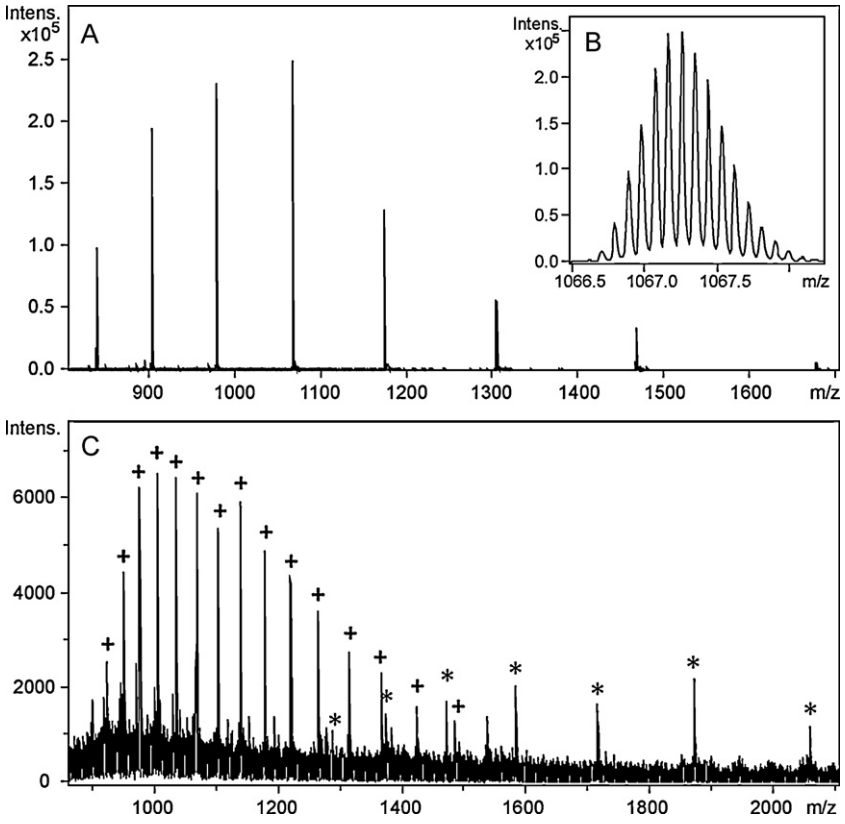

Fig. 4. Extracted mass spectra obtained for beta-2-microglobulin eluting at 67.3 min (A) with isotoptic resolution (charge is 11+) (B) and mass spectra of ubiquitin-conjugating enzyme E2 C(*) and annexin A5(+) that co-eluting at 89.4 min (C). LC conditions as described in Fig. 3.

a charge state of 39+. This mass corresponds with the molecular weight of serotransferrin (MW = 75,181 Da) that also contains two sialylated complex-type bi-antennary oligosaccharides (2 glycans each with a mass of 2206 Da) located at Asn^{432} and Asn^{630} [32].

The carbohydrate compositions outlined in Table 2 would be consistent with the observed deconvoluted mass spectrum for the serotransferrin depicted in Fig. 7B. The mass difference between peaks 1 and 2 (288.4 Da) is indicative of the loss of a single sialic

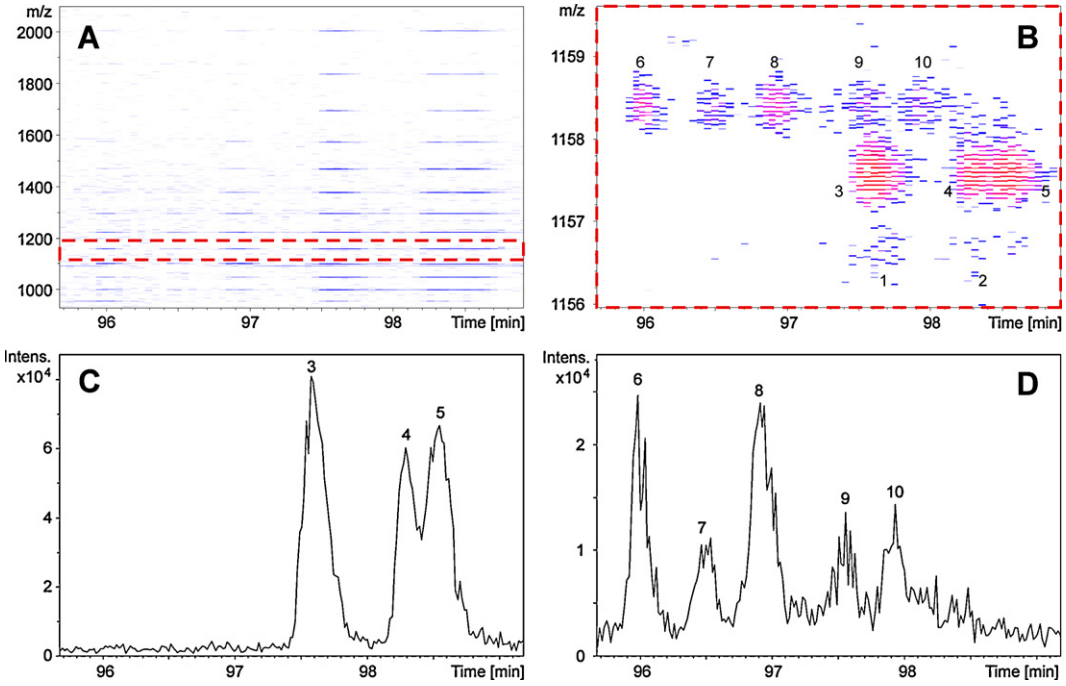

Fig. 5. Zoom-in density views (A and B) and extracted ion chromatograms (C and D) showing protein isoforms of peroxiredoxin 1 that differ in their oxidation state and place where oxidation occurs. Native peroxiredoxin 1 is represented by peaks 1–2; peaks 3–5 represent singly oxidized peroxiredoxin 1 protein isoforms; peaks 6–10 contain doubly oxidized peroxiredoxin 1. LC conditions as described in Fig. 3.

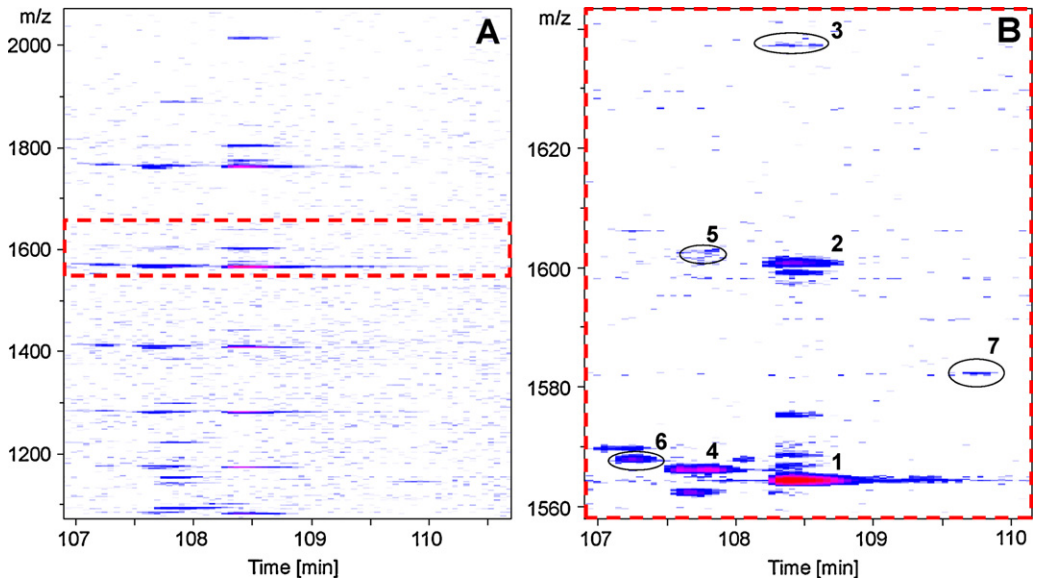

Fig. 6. Zoom-in density views of showing the charge envelope (A) and protein isoforms of alpha-lactalbumin (B). Peak (1) represents the native alpha-lactalbumin (2) and (3) alpha-lactalbumin containing one and two biotin tags, respectively, (4) alpha-lactalbumin containing one methionine or cystine oxidation, (5) alpha-lactalbumin containing one biotin tag and one oxidation, (6) alpha-lactalbumin containing two oxidations, and (7) alpha-lactalbumin containing a hexose monosaccharide residue. LC conditions as described in Fig. 3.

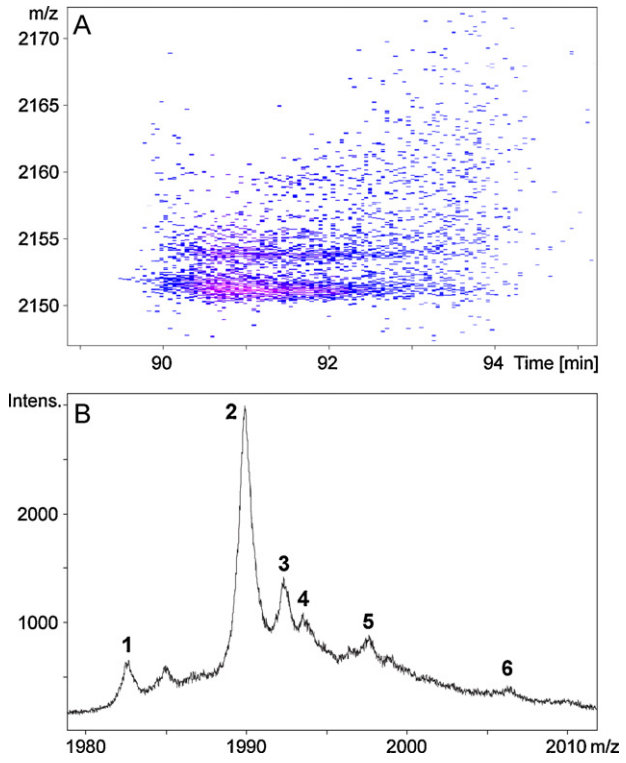

Fig. 7. Zoom-in density view and mass spectrum of the 39+ ion of serotransferrin showing the presence of N-glycosylation microheterogeneity. Peak interpretation in provided in Table 2 and discussed in the text. LC conditions as described in Fig. 3.

Table 2
Mass data and possible monosaccharide composition for N-glycosylated isoforms of serotransferrin.

Peak	ΔM_r (Da)		NeuAc	Fucose	Hexose	HexNAc
	Measured	Calculated				
1	–	–	3	0	10	8
1–2	290	291	4	0	10	8
2–4	144	146	4	1	10	8
4–5	165	162	4	1	11	8

acid (NeuAc, with an average calculated monosaccharide residue mass of 291.3 Da). The mass difference between peaks 2 and 4 is likely due the addition of a fucose monosaccharide residue (average mass: 146.1 Da) that can be linked to a HexNAc residue. The mass difference between peaks 4 and 5 is indicative of the addition of a hexose monosaccharide residue (average mass: 162.1 Da). Peaks 3 and 6 are likely serotransferrin isoforms. The mass difference between these two peaks (ΔM = 554.2 Da) may be explained by the presence of two HexNAc residues (N-acetylgalactoseamine or N-acetylglucoseamine) and one fucose monosaccharide residues (combined calculated average mass is 552.5 Da). Clearly not all isoforms in Fig. 7B could be elucidated. This is due the well-known microheterogeneity of N-glycans.

4. Conclusions

The limitations and possibilities of the LC–TOF-MS employing a 250 mm long monolithic capillary column for the analysis of intact proteins have been demonstrated using the ABRF 48 protein standard mixture. The method allowed for the chromatographic high-resolution separation of intact proteins at sensitivity levels that would make this method suitable for the analysis of samples of biological origin. Protein identification, based on comparison of the experimentally determined molecular weight with theoretical masses was tentative. This is the major drawback of this approach to data analysis, making it unsuitable for the analysis of actual biological samples. Albeit, this may be overcome by the application of MS/MS fragmentation techniques that are suitable for the analysis of large polypeptides, such as electron capture dissociation (ECD) on FTICR mass spectrometers or collision induced dissociation (CID) on ion-trap, ion-trap–orbitrap or QqTOF mass spectrometers. The combination of monolith technology and high-resolution TOF mass spectrometry presented, provides unique resolution to distinguish proteins isoforms arising from various modifications, including oxidation and biotinylation. The six most abundant protein isoforms due to glycosylation of serotransferrin could be tentatively identified. However, to tackle the microheterogeneity of N-glycans more efficient separations are required. We are planning to test if chromatographic performance could be improved using longer monolithic columns in combination with ultra-high-

pressure chromatography equipment. Also, we want to combine this with ETD-based top-down sequencing, aiming to achieve protein identification in the same experiment.

Acknowledgements

Support of this work by a grant of the Research Foundation Flanders (G.0919.09) is gratefully acknowledged. Dionex Corporation is acknowledged for financial support. NEPAF is a CELS project funded by ONE NorthEast and partly financed by the European Regional Development Fund (ERDF).

Appendix A. Supplementary data

Supplementary data associated with this article can be found, in the online version, at doi:10.1016/j.chroma.2011.06.049.

References

[1] A. Monzo, E. Sperling, A. Guttman, Trends Anal. Chem. 28 (2009) 854.
[2] S. Putz, J. Reinders, Y. Reinders, A. Sickmann, Expert Rev. Proteomics 2 (2005) 381.
[3] F.W. McLafferty, K. Breuker, M. Jin, X. Han, G. Infusini, H. Jiang, X. Kong, T.P. Begley, FEBS Lett. 274 (2007) 6256.
[4] K. Breuker, M. Jin, X. Han, H. Jiang, F.W. McLafferty, J. Am. Soc. Mass Spectrom. 19 (2008) 1045.
[5] A. Armirotti, U. Benatti, G. Damante, Rapid Commun. Mass Spectrom. 23 (2009) 661.
[6] D.J. Watson, S.A. McLuckey, Int. J. Mass Spectrom. 255 (2006) 53.
[7] H.J. Cooper, K. Hakansson, A.G. Marshall, Mass Spectrom. Rev. 24 (2005) 201.
[8] V.H. Wysocki, K.A. Resing, Q.F. Zang, G.L. Cheng, Methods 35 (2005) 211.
[9] G.C. McAllister, D. Phanstiel, D.M. Good, W.T. Berggren, J.J. Coon, Anal. Chem. 79 (2007) 3525.
[10] J. Wiesner, T. Presmsler, A. Sickmann, Proteomics 8 (2008) 4466.
[11] J.W. Eschelbach, J.W. Jorgenson, Anal. Chem. 78 (2006) 1697.
[12] A. Greider, L. Trojer, C.W. Huck, G.K. Bonn, J. Chromatogr. A 1216 (2009) 7747.
[13] P.A. Levkin, S. Eeltink, T.R. Stratton, R. Brennen, K. Robotti, H. Yin, K. Killeen, F. Svec, J.M.J. Fréchet, J. Chromatogr. A 1200 (2008) 55.
[14] Y.Y. Li, H.D. Tolley, M.L. Lee, Anal. Chem. 81 (2009) 9416.
[15] E.J. Sneekes, J. Hun, M. Elliot, J. Ausio, C. Borchers, J. Sep. Sci. 32 (2009) 2691.
[16] G. Holzl, H. Oberacher, S. Pitsch, A. Stutz, C.G. Huber, Anal. Chem. 77 (2005) 673.
[17] H. Oberacher, W. Parson, P.J. Oefner, B.M. Mayr, C.G. Huber, J. Am. Soc. Mass Spectrom. 15 (2004) 510.
[18] A.R. Ivanov, L. Zang, B.L. Karger, Anal. Chem. 75 (2003) 5306.
[19] S. Eeltink, L. Geiser, F. Svec, J.M.J. Fréchet, J. Sep. Sci. 30 (2007) 2814.
[20] S. Eeltink, S. Dolman, R. Swart, M. Ursem, P.J. Schoenmakers, J. Chromatogr. A 1217 (2010) 6610.
[21] M. Petro, F. Svec, I. Gitsov, J.M.J. Fréchet, Anal. Chem. 68 (1996) 315.
[22] A. Vellaichamy, J.C. Tran, A.D. Catherman, J.E. Lee, J.F. Kellie, S.M.M. Sweet, L. Zamdborg, P.M. Thomas, D.R. Ahlf, K.R. Durbin, G. Valaskovic, N.L. Kelleher, Anal. Chem. 82 (2010) 1234.
[23] Q.C. Wang, F. Svec, J.M.J. Fréchet, J. Chromatogr. A 669 (1994) 230.
[24] C.G. Huber, W. Walcher, A. Timperio, S. Trojani, A. Porceddu, L. Zolla, Proteomics 4 (2004) 3909.
[25] X. Yang, L. Ma, P.W. Carr, J. Chromatogr. A 1079 (2005) 213.
[26] S. Eeltink, S. Dolman, F. Detobel, G. Desmet, R. Swart, M. Ursem, J. Sep. Sci. 32 (2009) 2504.
[27] J. Mohr, R. Swart, M. Samonig, G. Bohm, C.G. Huber, Proteomics 10 (2010) 3598.
[28] F. Detobel, K. Broeckhoven, J. Wellens, B. Wouters, R. Swart, M. Ursem, G. Desmet, S. Eeltink, J. Chromatogr. A 1217 (2010) 3085.
[29] L. Bianco, J.A. Mead, C. Bessant, J. Proteome Res. 8 (2009) 1782.
[30] Z.A. Wood, E. Schro, J.R. Harris, L.B. Poole, Trends Biochem. Sci. 28 (2003) 32.
[31] I. Colas, O. Kololeva, P.J. Shaw, Plant Biosyst. 144 (2010) 703.
[32] Y. Satomi, Y. Shimonishi, T. Takao, FEBS Lett. 576 (2004) 51.